

# Nonlinear Spectroscopy of Cold Cesium in a Magneto-Optical Trap\*

J. W. R. Tabosa

*Departamento de Física, Universidade Federal de Pernambuco  
Cidade Universitária, 50739 Recife, PE, Brasil*

G. Chen, Z. Hu, R. B. Lee and H. J. Kimble

*Norman Bridge Laboratory of Physics 12-33  
California Institute of Technology, Pasadena, CA 91125*

Received June 22, 1992

In this paper we present an overview of recent results on nonlinear spectroscopy of cold atoms. Probe-beam amplification and absorption spectra are reported for cesium atoms cooled and confined in a magneto-optical trap. In addition to the well known spectrum of Mollow, novel spectral features with subnatural linewidths and single-pass gain of 20% are also observed. These narrow resonances can be qualitatively understood in terms of stimulated Raman processes in a three-level system. Negative radiation pressure is demonstrated as a mechanical consequence of optical gain.

## I. Introduction

Since the first proposal in 1975 by Hansch and Schawlow<sup>1</sup> of using laser light to cool an atomic sample, there has been a dramatic progress in the area of laser cooling and trapping of neutral atoms<sup>2,3</sup>. The possibility of obtaining high densities of cold atoms and the understanding of the intrinsic physical process leading to low temperatures were the principal motivations for the most part of groups involved in this field. From a spectroscopic point of view, the capability of producing dense samples of cold atoms allows spectroscopic investigation; in a domain where Doppler and transit broadening can be greatly reduced, which could also be important for many quantum optics experiments.

From an alternate perspective, spectroscopic characterizations of trapped atoms can provide important new information about the dynamics of the trap itself, as has been demonstrated in recent absorption spectra of cold and confined atoms<sup>4,5</sup>.

In this paper, we present a detailed spectroscopic investigation of trapped cesium atoms in a magneto-optical trap, described in the following section. We report measurements of the spectral response of the cold sample to a weak probe beam for a range of detunings and saturating power of the beams that form the trap. The recorded transmission spectra for the probe beam reveal the presence of broad absorption and gain which are in reasonable agreement with earlier spectra calculated by Mollow<sup>6</sup> for a two-level atom in a strong field.

For strong saturation, Mollow's spectrum can present gain, which can be interpreted as originated by stimulated transitions between dressed-states with inverted population. However, novel narrow spectral features around the frequency of the trapping beams are also observed, which can be qualitatively understood in terms of Raman resonances in a three-level system. This feature has a width well below the natural linewidth and can present an appreciable single pass gain. We also explore the correlation between this narrow spectral feature and the mechanical properties of the trapped atoms and show that this can lead to the observation of both positive and negative radiation pressure, associated with stimulated absorption and emission from and into the probe beam, respectively.

## II. The Magnetic Optical Trap (ZOT)

One of the most successful optical traps was the so called Zeeman-shift spontaneous force optical trap (ZOT) or magneto-optical trap, first demonstrated by Raab et al in 1987<sup>7</sup>. It is a very deep optical trap and has been used to achieve densities of cold atoms<sup>3</sup> higher than  $10^{11}$  atoms/cm<sup>3</sup>. However, for the experimental realization of previously built optical traps, including the ZOT, a voluminous ultra-high vacuum apparatus was required, due to the "necessity" of first slowing down an atomic beam prior to trapping. An exciting development in this field was the recent demonstration by a group at the University of Colorado<sup>8</sup> of the trapping of neutral atoms directly from an atomic vapor in a cell at room temperature. In this case the trap

\*A preliminary version of this work has been presented at the one-day Workshop on Nonlinear and Quantum Optics (Recife, February 1992).

is filled with the slow velocity atoms in the tail of the Maxwellian velocity distribution, and while the optical arrangement is the same as in the former ZOT, this cell-trap represents an enormous simplification in the experimental apparatus, allowing now the possibility of obtaining samples of ultra-cold atoms even in small laboratories.

Although this trap can work for atoms with a complicated hyperfine structure, the basic principle can be illustrated by considering a hypothetical atom with total angular momentum  $F = 0$  and  $F = 1$  for ground and excited state respectively (as for example in the hyperfine structure). The atoms are placed in a weak magnetic field  $B(z) = (\frac{dB}{dz})z$ , so that the degenerated Zeeman sublevels are split by the field gradient according to Figure 1. The atoms are illuminated by a pair of counterpropagating laser beams, with opposite circular polarization  $\sigma^+$  and  $\sigma^-$  and frequencies  $\omega_L$  detuned below the unshifted  $m_F = 0$  resonance frequency. It is easy to see that at the point with zero magnetic field ( $z = 0$ ) the force from the two beams will exactly cancel. However if the atoms moves to a position  $z > 0$  it will absorb more light from the  $\sigma^-$  beam, than from the  $\sigma^+$  beam, since for  $z > 0$  the Zeeman shifted  $m_F = -1$  level is closer to resonance than the level  $m_F = 1$ . The atom is then pushed back to the origin  $z = 0$ . On the other hand at a position  $z < 0$  the Zeeman shift is reversed, so the force is again directed towards the origin  $z = 0$ .

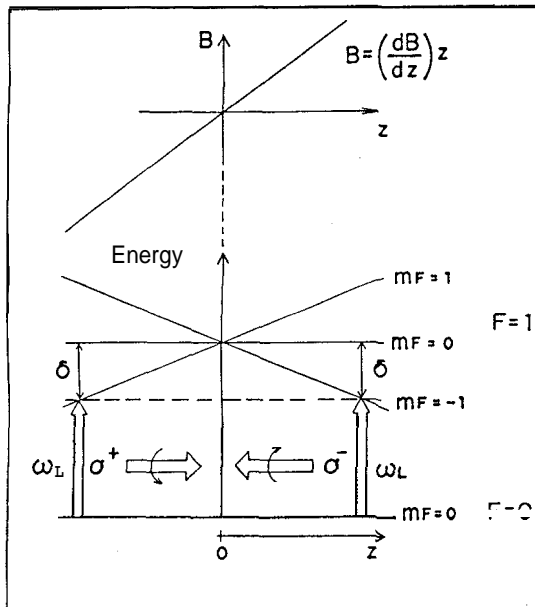


Figure 1.: Zeeman shifted energy-level for a  $F = 0 \rightarrow F = 1$  transition to illustrate the operation of the ZOT.

To make this discussion more quantitative in this simple case, we can calculate the net force on a single atom. Let us assume that the two beams shown in Fig.1 are plane waves and have the same intensity. If we consider the low intensity limit, so that the beams

do not saturate the atomic transition, it is possible to add independently the force created by each laser beam. Thus, the net force on an atom moving with velocity  $v$ , is given by

$$\vec{F} = \vec{F}_{\sigma^+} + \vec{F}_{\sigma^-} \quad (1)$$

where,

$$\vec{F}_{\sigma^\pm} = \pm \frac{1}{2} \hbar \vec{K} \gamma \frac{\Omega^2/2}{(\delta \mp K v_z \mp \Delta)^2 + \frac{\gamma^2}{4}} \quad (2)$$

In the equation (2)  $\gamma$  is the natural linewidth,  $\delta = \omega_L - \omega_0 < 0$  is the detuning between the laser frequency and the unshifted atomic frequency,  $\vec{K}$  is the wavevector,  $\Omega$  is the Rabi frequency ( $\Omega = \mu E/\hbar$ , where  $E$  is the amplitude of the electric field and  $\mu$  is the transition dipole moment) and  $A = \mu_m \frac{dB}{dz} z/\hbar$  ( $\mu_m$  being the magnetic dipole moment for the excited state) is the Zeeman shift in the atomic frequency.

If we take the limit of low atomic velocities and small Zeeman shift [ $(|\delta| \sim y) \gg |k v_z|, |\Delta|$ ], the force can be rewritten as

$$F = -\tilde{\gamma} v_z - \tilde{K} z, \quad (3)$$

with

$$\tilde{\gamma} = -\frac{\hbar \gamma \Omega^2 \delta K^2}{(\delta^2 + \gamma^2/4)^2}, \quad (4)$$

and

$$\tilde{K} = -\frac{K \gamma \Omega^2 \delta \mu_m \frac{dB}{dz}}{(\delta^2 + \gamma^2/4)^2} \quad (5)$$

Since  $\delta < 0$ , in this limit the atom will be driven by a force which has a damping term, responsible for cooling and a restoring term, responsible for trapping the atoms. The equation of motion for an atom with mass  $m$  is simply that of a damped harmonic oscillation,  $\ddot{z} + 2\beta\dot{z} + \omega^2 z = 0$ , where  $\beta = \tilde{\gamma}/2m$  is the damping rate and  $\omega = \sqrt{\frac{\tilde{K}}{m}}$  the natural frequency. If we consider cesium atoms ( $\lambda = 852nm$ ), with  $\delta = \gamma/2$ ,  $\Omega^2/\gamma^2 = 0.1$  and  $\frac{dB}{dz} = 10 \text{ G/cm}$ , we find that  $\beta^2/\omega^2 \sim 5$ , which show that, in fact, this corresponds to an overdamped harmonic oscillator.

Extension of this scheme to three dimensions can be easily made by adding two more pairs of counterpropagating beams in the X and Y direction and employing a spherical magnetic quadrupole which will provide confinement along these directions.

Although we have considered here the low intensity limit, the trap also works when the laser beams are so strong that the atomic transition is saturated. In particular, this is a very interesting experimental situation

to study the atom-field interaction, without having to take in account the velocity distribution.

### III. Experimental Results

Our experiment employs atomic cesium in a magneto-optical trap as illustrated in Figure 2. The trap is loaded directly from cesium vapor in a quartz cell with a square cross section of  $1\text{cm}^2$ . The cell is illuminated by three counterpropagating pairs of laser beams of opposite circular polarization arranged along mutually orthogonal directions and with common frequency tuned several natural linewidths below the resonant transition ( $6S_{1/2}, F = 4 \rightarrow 6P_{3/2}, F' = 5$ ) at  $852\text{nm}$ . A spatially dependent trapping force arises from the position dependence of the atomic Zeeman shift in an inhomogeneous magnetic field of gradient of  $10\text{G/cm}$  along  $z$  and  $5\text{G/cm}$  along  $(x, y)$  created by two current carrying coils. In the steady state, the number of trapped atoms is determined by the balance of laser capture from and collisional loss with the background of Cs vapor in the cell. The typical filling time of the trap following a sudden turn on of the trapping lasers is about  $1\text{s}$  for a cell with Cs pressure  $2 \times 10^{-8}\text{Torr}$ , with the diameter of the steady state cloud of trapped Cs atoms being about  $1\text{mm}$ . The temperature of the trapped atoms is near the Doppler cooling limit ( $125\mu\text{K}$ ) as inferred by monitoring the decay in absorption of a weak probe beam when the trapping lasers are chopped off. In our experiments, the trapping beams are of waist  $\omega_0 = 4\text{mm}$  and are derived from a frequency stabilized  $\text{Ti} : \text{Al}_2\text{O}_3$  laser with linewidth below  $100\text{kHz}$ . Radiation from a semiconductor diode laser recirculates the population lost to the  $F = 3$  ground state.

Given this brief survey of the ZOT, we next turn to our spectroscopic study to investigate more explicitly the microscopic dynamics of the trap. Again with reference to Figure 2, under conditions of strong excitation by the trapping lasers, we record the transmitted power as a function of the frequency  $\omega_p$  for a low intensity probe beam of waist  $\simeq 100\mu\text{m}$  focused through the trap. The probe beam is derived from the  $\text{Ti} : \text{Al}_2\text{O}_3$  laser and is independently tuned over a limited range in frequency by acousto-optic modulators. Figure 3 is typical of our results for the probe spectra and is a succession of records of the transmitted probe power normalized to the input probe power ( $p/p_0$ ) versus  $\omega_p$ , with the positions of the frequencies of the trapping laser  $\omega_T$  and of the atomic transition  $\omega_A$  indicated. As might be expected<sup>6</sup>, we observe in Fig.3a the probe spectrum with broad regions of absorption and amplification symmetrically placed about  $\omega_T$ , characteristic of the dressed-state splitting. However, in addition to the broad features, a narrow dispersive-shaped feature around  $\omega_T$  is also clearly evident in Figure 3a. This narrow feature has a width below the natural linewidth

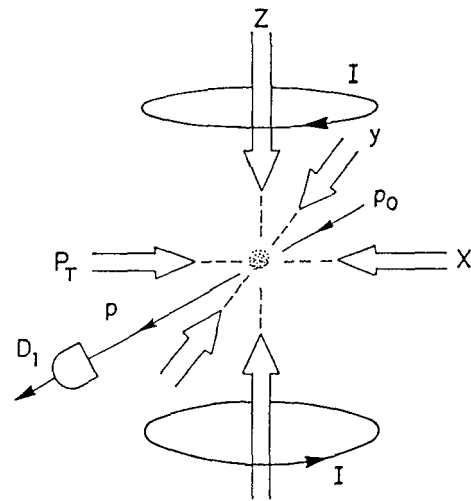


Figure 2.: Experimental arrangement of the trap (ZOT).

of  $\gamma_{\perp}/\pi = 5\text{MHz}$  and can exhibit appreciable single-pass gain ( $> 20\%$ ). An expanded view of the absorption spectrum is given in Figure 3b-d, where we see that for increasing levels of trapping power  $P_T$ , the dispersive shape broadens and develops a substructure. The general trends shown in Figure 3 are independent of the number of trapped atoms as well as of the direction of propagation of the probe beam relative to the trapping beams. However, the spectra do exhibit a dependence on the polarization state of the incident probe beam (especially as regards the substructure shown in Figure b-d and on the magnetic field gradient across the trap ( $\Delta B \sim 1\text{G}$  gives a range  $\Delta\omega_A/2\pi \sim 1\text{MHz}$ ). For example, for a fixed trapping power ( $1.6\text{mW}$ ), Figure 4 shows the narrow feature for two different values of the magnetic field gradient. As we can see, the shape of the narrow feature changes and the ratio between the sizes of gain and absorption parts seems to decrease with the magnetic field. However, the interpretation of these results require that we take into account modifications in the morphology of the trap.

To model these probe spectra, we can make some headway by first of all attempting to assess the role of the multiplicity of Zeeman transitions with a crude adaptation of the standard two-state result<sup>6</sup>. Our approach is to average the absorption spectra for a weak probe over the distribution of dipole moments for the  $F = 4 \rightarrow F' = 5$  transition in Cs. Pursuing this analysis somewhat further, we present in Figure 5 a compilation of results such as in Fig.3a over a range of trapping power  $0 \leq P_T \leq 3\text{mW}$ . With regard to the splitting  $\Omega$  between  $\omega_T$  and the broad absorption feature, we find that the average over Zeeman sublevels does not produce significant departures from the two-state result.

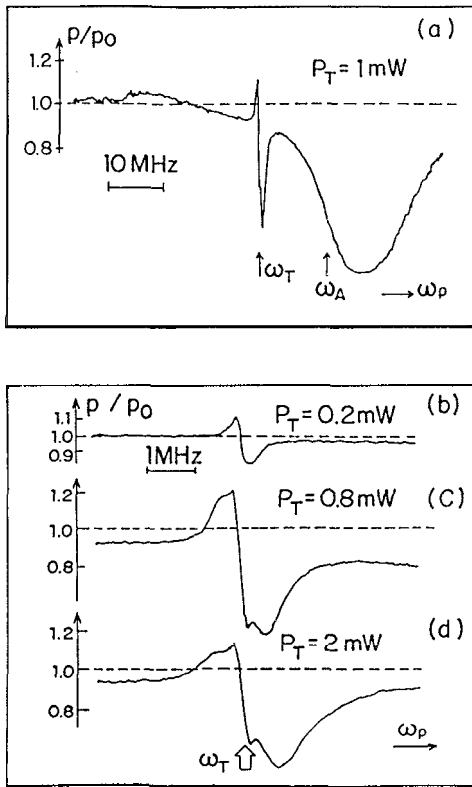


Figure 3.: Probe absorption spectra  $p/p_0$  versus probe frequency  $\omega_p$  for  $(\omega_A - \omega_T)/2\pi = 13.5$  MHz. (a) Scans showing large absorption near  $\omega_A$  and small gain symmetrically placed about  $\omega_T$ . (b-d) Magnified frequency scale to examine the narrow central feature near  $\omega_T$  for various  $P_T$ .

By contrast, the large spread in Clebsch-Gordan coefficients within the  $F = 4 \rightarrow F' = 5$  manifold results in a broadening that substantially increases the width  $\beta$  above the two-state result for both the experimental scans and the calculation. That this excess width does not arise from heating of the trap with increasing  $P_T$  has been established with measurements both of the transient decay of the trap and of the probe spectrum with a chopping technique that leads to the points for  $(\tilde{\Omega}, \beta)$  at  $R = 0$ . Note that in Figure 5,  $R$  is referenced to the  $m_F = 4 \rightarrow m'_F = 5$  transition with  $R = 1$  for  $\mathbf{I} \approx 1 \text{ mW/cm}^2$ , where  $\mathbf{I} = 6I_T$  and  $I_T = 2P_T/\pi\omega_0^2$ . The set of theoretical Rabi frequencies has been scaled by  $a = 0.85$  ( $R \rightarrow a\Omega$ ) to optimize the comparison.

If we next consider the narrow central feature near  $\omega_T$ , we might attempt to account for the rather complex optical pumping processes within the manifold of Zeeman states with an extension of the usual two-state calculation to include relaxation to and from neighboring Zeeman transitions. As opposed to our previous summation, such approach for an "open" two-state sys-

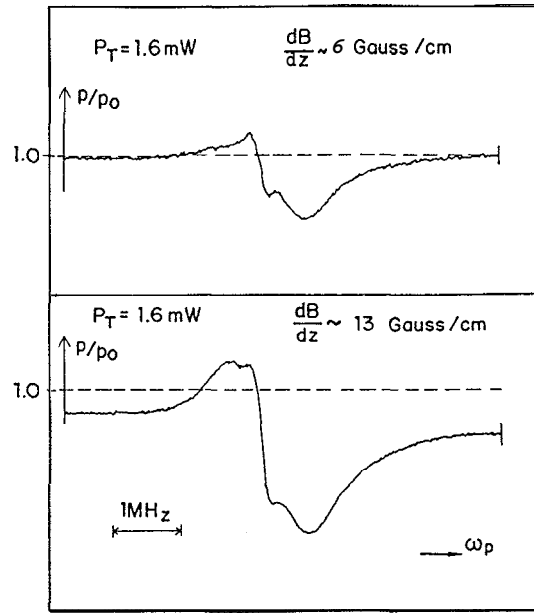


Figure 4.: Narrow feature absorption spectra for two different values of the magnetic-field gradient.

tem offers the possibility for describing certain dynamical aspects of the problem, as for example the differential rate of relaxation of ground and excited state populations<sup>10,11</sup>. Unfortunately, the spectrum for the "open" two-state system exhibits either very small central features of the same symmetry as in Figure 3 or larger features of size comparable to our data but of opposite symmetry<sup>9-11</sup>.

Another avenue that we have followed is to calculate the spectra using a three-level  $\Lambda$  system for which slow relaxation between ground states can lead to narrow spectral features<sup>12-17</sup>. If we consider the three-level  $\Lambda$  system shown in the inset of Figure 6 driven by two pump fields of common frequency  $\omega'$ , but interacting with different transitions, then it is easy to see that a stimulated Raman process leads to amplification of the probe beam when  $\omega' - \omega_p = \delta'$  and to absorption when  $\omega' - \omega_p = -\delta'$ , where  $\delta'$  is the frequency splitting of the ground states. This is because the steady state population of level 2 exceeds that of level 3. In the correspondence of this model with the experiment, the differential detuning  $\delta'$  can be due to the range of Doppler shifts, the spatially-dependent Zeeman splitting across the trap or the light-shifts, while a mixing of ground states might be driven by atomic motion through the polarization gradients of the trap. For appropriate choices of decay rates and Rabi frequencies, we can obtain spectra qualitatively similar to those observed in the experiment. Figure 6 shows one of such spectrum, for the parameters given in the inset. Although this model is encouraging for weak fields, un-

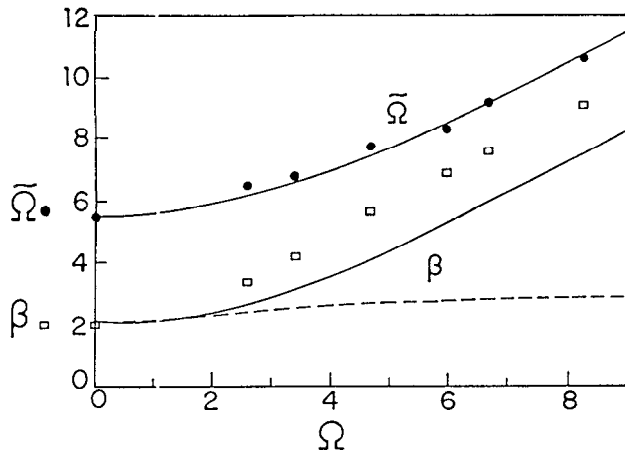


Figure 5.: Frequency splitting  $\tilde{\Omega}$  ( $\bullet$ ) and width  $\beta$  ( $\square$ ) of the broad absorption feature versus Rabi frequency  $\Omega$  of trapping beams for  $(\omega_A - \omega_T)/2\pi = 13.5$  MHz. Theoretical curves for  $(\tilde{\Omega}, \beta)$  are from an average for  $F = 4 \rightarrow F' = 5$ . The dashed curve gives  $\beta$  for the single two-state transition; a similar curve for  $\tilde{\Omega}$  would roughly overlay the multistate result. The normalization for  $(\tilde{\Omega}, \beta)$  is  $\gamma_{\perp}/2\pi = 2.5$  MHz; for  $\Omega$  it is  $\sqrt{2}\gamma_{\perp}$ .

fortunately for strong excitation as in Figures 3,4, the calculated absorption spectra depart significantly from our experimental traces as the field-dependent dressed states for the A-system emerge.

The decidedly mixed scorecard for the above analysis leads us to conclude that a detailed understanding of the absorption spectra will likely require a complex treatment of the relevant cesium levels together with the microscopic environment of the trap.

#### IV. Mechanical Effects in the Trap

As we discussed in the previous section, our view is that atomic motion inside the trap environment plays an important role for the understanding of the observed spectra. For example, for an atom moving with the averaged thermal speed in the trap ( $v \sim 10$  cm/s), the polarization gradient created by the six laser beams will produce a coherent modulation in the Zeeman population varying with a rate comparable to the observed width of the narrow feature.

Not surprisingly then, our measurements of absorption spectra bring us full circle back to the difficult question of the self-consistent relationship between the spectroscopic and mechanical characteristics of the trap. To begin to address this issue, we present in Figure 7 a series of images that illustrate a correlation between the narrow spectral resonances and the morphology of the trap. Figure 7a is a relatively symmetric picture of the trapped cloud of Cs atoms in the absence of the probe beam. In Figure 7b the probe beam is present and it

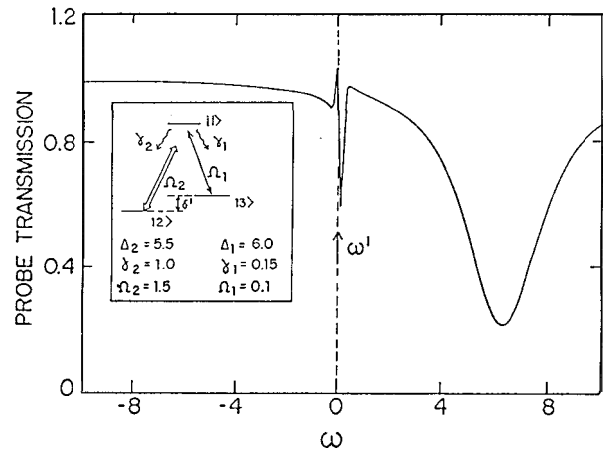


Figure 6.: Calculated absorption spectrum for the A three-level system showed in the inset.  $\Omega_{1,2}$  are the Rabi frequencies associated with each pump field,  $\gamma_{1,2}$  the relaxations rates, and  $\Delta_{1,2}$  the corresponding laser detuning.

is tuned for absorption in the narrow feature in Figure 3. In this case the atoms in the trap recoil along the direction of propagation of the probe beam (stimulated absorption resulting in positive radiation pressure). In Figure 7c the probe frequency is tuned into the region of gain in the subnatural profile, with the result that the atoms in the trap recoil opposite to the direction of propagation of the probe beam (stimulated emission resulting in "negative" radiation pressure)<sup>18</sup>. While our demonstration is with an externally applied probe, the atomic fluorescence itself serves as a self-generated probe which couples internal spectroscopic and external mechanical degrees of freedom. For example, atoms with velocities with  $Kv > 0$  will experience one type of force, while those with  $Kv < 0$  will experience another. So, beyond the remarkable demonstration of negative radiation pressure, Fig.7 serves to illustrate the importance of take into account the existing correlation between the spectroscopy and mechanical motion in the trap. From another perspective, negative radiation pressure can be employed to optically implode<sup>19</sup> the trapped sample, as suggested in reference<sup>4</sup>.

#### V. Conclusions

We have described an investigation of the nonlinear spectroscopy of cesium atoms cooled and confined in a magneto-optical trap. Novel spectral features with subnatural linewidth were observed and qualitatively explained in terms of stimulated Raman resonances in a A-three-level system involving different m-levels. We also demonstrate that the mechanical effect of optical gain leads to the observation of negative radiation pressure and have showed the importance of the coupling

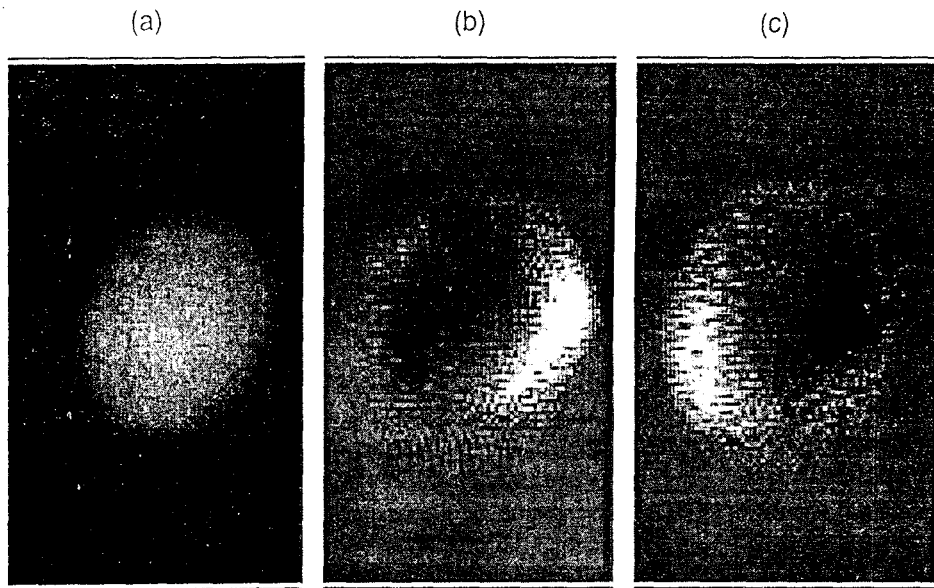


Figure 7.: Images of trapped Cesium atoms viewed from  $[110]$  direction (Figure 2). (a) Trap in the absence of the probe beam with radius  $R \sim 0.4mm$ . (b-c) Trap with probe beam propagating from left to right and into the page by about  $25^\circ$  (along  $[1,3,0]$  direction). (b) Probe detuning  $(\omega_p - \omega_T)/2\pi \simeq +0.3$  MHz, with recoil along the direction of probe propagation (absorption). (c) Probe detuning  $(\omega_p - \omega_T)/2\pi \simeq -0.3$  MHz, with recoil opposite to the direction of probe propagation (gain). In (b,c), the images shown are the difference between (a) and the corresponding image in the presence of the probe beam, with light (dark) indicating an increase (decrease) in atomic fluorescence

between the spectroscopic and mechanical properties of the trap, for the complete understanding of the observed spectra. This understanding could give us important information about how the trap really works. On the other hand, as we already pointed out, a cloud of cold and trapped atoms is an exciting system for many quantum optics investigations. In particular, we will try to observe noise reduction in four-wave mixing oscillation in an optical cavity, using cold atoms as the nonlinear medium.

This work was supported by the National Science Foundation, by Venture Research International, by the Office of Naval Research, and by CNPq - Conselho Nacional de Desenvolvimento Científico e Tecnológico - Brazil (JWRT). We are grateful to Professors C. Wieman and T. Walker whose generosity helped to initiate this program and to Professor K. Libbrecht for important contributions.

## References

1. T. W. Hansch and A. L. Schawlow, *Opt. Commun.* **13**, 68 (1975).
2. *Laser Cooling and Trapping of Atoms*, Eds. S. Chu and C. Wieman, *J. Opt. Soc. Am.* **B6**, 2020 (1989).
3. D. W. Sesko, T. G. Walker and C. Wieman, *J. Opt. Soc. Am.* **B8** 946 (1991); A. M. Steane and C. J. Foot, *Europhys. Lett.* **14**, 231 (1991).
4. J. W. R. Tabosa, G. Chen, Z. Hu, R. B. Lee and H. J. Kimble, *Phys. Rev. Lett.* **66**, 3245 (1991).
5. D. Grison, B. Lounis, C. Salomon, J.Y. Courtois and G. Grynberg, *Europhys. Lett.* **15**, 149 (1991).
6. R. R. Mollow, *Phys. Rev.* **A5**, 2217 (1972); F.Y. Wu et al, *Phys. Rev. Lett.* **38**, 1077 (1977); Mark T. Gremisen et al, *J. Opt. Soc. Am.* **B5**, 123 (1987).
7. E. L. Raab, M. G. Prentiss, A. E. Cable, S. Chu and D. E. Pritchard, *Phys. Rev. Lett.* **59**, 2631 (1987).
8. C. Monroe, W. Swann, H. Robinson and C. Wieman, *Phys. Rev. Lett.* **65**, 1591 (1990).
9. Y. Shevy, *Phys. Rev. A* **41**, 5229 (1990).
10. A. D. Wilson-Gordon and H. Friedmann, *Opt. Lett.* **14**, 390 (1989).
11. G. Khitrova, P. R. Rernan and M. Sargent III, *J. Opt. Soc. Am.* **B5**, 160 (1987).
12. *Nonlinear Laser Spectroscopy*. V. S. Letokhov and V. P. Chebotayev. (Springer-Verlag, Berlin, 1977). Ch.5.
13. G. Orriols, *Il Nuovo Cimento* **53**, 1 (1979).
14. G. S. Agrawal and S. S. Jha, *J. Phys. B* **12**, 2655 (1979).
15. R. M. Whitley and C. R. Stroud, *Phys. Rev. A* **14**, 1498 (1976).

16. C. Coher-Tannoudji and S. Reynaud, J. Phys. B 10, 2311 (1977).
17. L. M. Narducci, M. D. Scully, G.-L. Oppo and J. R. Tredicce, Phys. Rev. A 42, 1630 (1990).
18. The probe intensity  $I$ , for Figure 7 is about  $4mW/cm^2$ , while Figure 3 is taken with  $I$ , below  $0.4mW/cm^2$  so that the spectra are independent of the probe power and do not exhibit such large recoil.
19. J. Dalibard, Opt. Commun. 68, 203 (1988).